Rapid Stiffening of Integrin Receptor-Actin Linkages in Endothelial Cells Stimulated with Thrombin: A Magnetic Bead Microrheology Study

Andreas R. Bausch,* Ulrike Hellerer,* Markus Essler,† Martin Aepfelbacher,‡ and Erich Sackmann*
*Physik Department E22 (Biophysics group), Technische Universität München, D-85748 Garching; †Max von Pettenkofer Institut für Medizinische Mikrobiologie, Universität München, Pettenkoferstr. 9a, 80336 München, ‡Instutut für Prophylaxe und Epidemiologie der Kreislaufkrankheiten, Universität München, Pettenkoferstr. 9, D-80336 München, Germany

ABSTRACT By using magnetic bead microrheology we study the effect of inflammatory agents and toxins on the viscoelastic moduli of endothelial cell plasma membranes in real time. Viscoelastic response curves were acquired by applying short force pulses of ~500 pN to fibronectin-coated magnetic beads attached to the surface membrane of endothelial cells. Upon addition of thrombin, a rapid stiffening of the membrane was observed within 5 s, followed by recovery of the initial deformability within 2 min. By using specific inhibitors, two known pathways by which thrombin induces actin reorganization in endothelial cells, namely activation of Ca^{2+}-calmodulin-dependent myosin light chain kinase and stimulation of Rho/Rho-kinase, were excluded as possible causes of the stiffening effect. Interestingly, the cytotoxic necrotizing factor of *Escherichia coli*, a toxin which, in addition to Rho, activates the GTPases Rac and CDC42Hs, also induced a dramatic stiffening effect, suggesting that the stiffening may be mediated through a Rac- or Cdc42Hs-dependent pathway. This work demonstrates that magnetic bead microrheometry is not only a powerful tool to determine the absolute viscoelastic moduli of the composite cell plasma membrane, but also a valuable tool to study in real time the effect of drugs or toxins on the viscoelastic parameters of the plasma membrane.

INTRODUCTION

Endothelial cell monolayers form semipermeable interfaces between blood vessels and surrounding tissues. The endothelial barrier function for macromolecules is tightly controlled by adhesion between adjacent cells, which is in turn mediated by adherens junctions consisting of homomultimeric interactions of cadherins and by integrins located at cell-cell contacts (Lampugnani et al., 1995). The integrity of the endothelial cell layer is also controlled by the tethering of the cells to the extracellular matrix through integrins. Integrins can be linked to the intracellular actin cytoskeleton by a large number of actin-binding proteins such as α-actinin, vinculin, talin, and paxillin (Yamada and Geiger, 1997). The tethering force can be strengthened by the formation of actin bundles (called stress fibers), which are connected to integrin clusters via actin-binding proteins. Through the formation of stress fibers, endothelial cells can drastically enhance their adhesion forces in order to resist shear strain in the blood vessel. Furthermore, these mechanisms have also been shown to modulate cell contraction by activation of the actin-myosin motor complex (Jalink et al., 1994; Allen et al., 1997; Aepfelbacher et al., 1996).

The integrity of endothelial cell layers plays a critical role for the maintenance of the barrier function of blood vessels. The effects of inflammatory agents and bacterial toxins on the shape, adhesion strength, and generation of mechanical forces of endothelial cells have motivated extensive studies (Garcia and Schaphorst, 1995). These studies provide detailed insight into the effect of these agents on the various signaling pathways that control the activity of the contractile actomyosin network.

One of the best-studied endothelial activators is thrombin, which is coupled via heterotrimeric G-proteins of the Gq-family to phospholipase C-β, which cleaves phosphatidylinositol-4,5-bisphosphate into inositol-1,4,5-trisphosphate and diacylglycerol. The former activates protein kinase C (PKC), and the latter releases Ca^{2+} from storage vesicles. Both PKC and Ca^{2+}-calmodulin-activated myosin light chain kinase can induce contraction of endothelial cells by direct phosphorylation of the light chain of myosin II (MLC). This pathway was shown recently to act in concert with another pathway, which is mediated by the G-protein Rho and controls the activity of the myosin light chain phosphatase. It was demonstrated that thrombin activates Rho, which stimulates its target Rho-kinase, causing phosphorylation and inactivation of MLC-phosphatase (Essler et al., 1998). Through these two pathways thrombin induces a radical reorganization of the actin cytoskeleton: new actin filaments are formed within seconds and numerous stress fibers form, which span the cell body. After ~2 min the cells contract and round up, due to centripetally acting forces, which have been studied by tensiometry (Bodmer et al., 1997).

In the present work we applied a recently developed magnetic tweezers microrheology technique to study the effect of thrombin on the coupling of the actin cytoskeleton to integrin receptors in real time (Bausch et al., 1998, 1999). Magnetic colloidal beads were coated with fibronectin and

Received for publication 1 September 2000 and in final form 8 March 2001.

Address reprint requests to Dr. Andreas R. Bausch, Technische Universität München, Lehrstuhl für Biophysik E22, James-Franck-Strasse, D-85748 Garching, Germany, Tel: 49-89-12471; Fax: 49-89-289-12469; E-mail: dbausch@physik.tu-muenchen.de.

© 2001 by the Biophysical Society

0006-3495/01/06/2649/09 $2.00

attached to the fibronectin receptors on the surface membrane of human umbilical vein endothelial cells (HUVEC). The local deformability of the cell membrane was measured repeatedly by analysis of the transient deflection of the beads induced by magnetic field pulses. These experiments provide information about the coupling of the endothelial cells to the bead surfaces via integrin and are thus also expected to yield insight about the tethering forces of the cells to substrates. They are thus complementary to studies of the permeability of endothelial cell layers or tensiometric measurements, which give insight into modifications of the cell-cell interactions in response to inflammatory agents (Bodmer et al., 1997; Kolodney and Wysolmerski, 1992).

We found a dramatic stiffening of the bead attached to the cell membrane after application of thrombin. The thrombin effect was abolished by cytochalasin D, demonstrating the involvement of actin polymerization, but was not affected by inhibitors of the Ca^{2+}/calmodulin or Rho/Rho-kinase pathways. Furthermore, we find that the cytotoxic necrotizing factor, a toxin that activates several Rho-GTPases in addition to Rho, also induced the stiffening response, suggesting the involvement of a Rho-independent mechanism for the coupling of actin to integrins.

The study demonstrates that for the first time, real-time measurements of the effect of hormones or drugs on the local mechanical properties of the endothelial plasma membrane are possible, using the magnetic bead microrheometry technique.

MATERIALS AND METHODS

Endothelial cells

HUVECs were obtained by cannulating segments of human umbilical cord veins, incubated with α-chymotrypsin (Sigma, Toufkitchen, Germany) for 30 min, and gently irrigated. The irrigant was collected and harvested cells were plated onto collagen-coated (collagen G consisting of 90% collagen I, 10% collagen III, Biochrom, Berlin, Germany) plastic culture flasks. HUVECs were cultured in EGM (Promo Cell, Heidelberg, Germany) containing ECGS/H2 (endothelial cell growth supplement/heparin) and 10% FCS at 5% CO_2 and 37°C in a humidified atmosphere. Before the experiment, HUVECs (4×10^4 cells) were plated onto collagen-coated coverslips and grown typically for 1–2 days. The glass coverslips (lateral dimensions 18×18 mm^2, Menzel Gläser, Germany) were washed before use with Hellmanex solution (Hellma GmbH, München, Germany) in a sonicator, rinsed several times with Millipore water, sterilized by washing in ethanol solution, and dried. Before use these coverslips were coated for 2 h or overnight with 100 μg/ml collagen G (Biochrom) and washed twice with phosphate-buffered saline (PBS, Sigma).

Functionalization of the Dynabeads

In all experiments super paramagnetic Dynabeads with a diameter of 4.5 μm (Dynal, Hamburg, Germany) were used. In order to allow coupling to integrin receptors, the beads were coated with plasma fibronectin (Life Technologies, Paisley, Scotland) or with collagen IV (Biochrom). Fibronectin and collagen IV were coupled to the reactive tosyl groups of the beads according to the procedure provided by the supplier.

Immediately before sample preparation, the functionalized magnetic beads were washed once in PBS and suspended in HEPES (Sigma) buffered cell medium. The bead concentration was adjusted to 10^5 beads/ml and the solution was added to the cells adherent to the coverglass. The cells were incubated with beads for 10 min and washed gently before mounting the coverglass on the sample holder of the magnetic bead rheometer.

Measuring chamber and force transducer

The measuring chamber and the magnet have been described in detail previously (Ziemann et al., 1994; Bausch et al., 1998). Briefly, the magnetic field is generated by a solenoid with a soft iron core exhibiting a nose with a sharp edge. The nose penetrates the measuring chamber and the distance between cells and the tip of the iron core can be adjusted to a value of $\sim$100 μm. This allows the application of local forces of up to 10 nN. The measuring chamber consists of a copper block into which an 18×18 mm^2 Teflon frame is fitted, which serves as a holder for the coverglass with the adhering cells. The measuring chamber contains 50–100 μl of solution, depending on the position of the iron core tip, and is not sealed at the top. A function generator triggers a custom-built amplifier to activate the magnetic solenoid. The magnet and the measuring chamber are mounted on the stage of a Zeiss Axiovert microscope. For the observation of the cells and the magnetic beads, phase contrast images are taken with a Zeiss Plan-Neofluar objective (40× PH 2) and a CCD camera (C3077, Hamamatsu Photonics, Hamamatsu City, Japan) connected to a VCR (WJ-MX30, Matsushita Electric Industrial Co., Osaka, Japan). The recorded sequences are digitized using an Apple Power Macintosh 9500 (Apple Computer, Cupertino, CA) equipped with an LG3 frame grabber card (Scion Corp., Frederick, MD). The position of the particles is determined with an accuracy of $\sim$10 nm using a self-written single particle tracking algorithm implemented in the public domain image processing software National Institutes of Health Image (National Institutes of Health, Bethesda, MD).

Visualization of actin network by microfluorescence

To label F-actin, cells were fixed for 10 min with 3.7% paraformaldehyde in PBS containing 1 mM Mg^{2+} and 0.1 mM Ca^{2+}, permeabilized in cold acetone (−20°C) for 5 min, and air-dried. Coverslips were washed three times, incubated for 20 min with Alexa phalloidin (Molecular Probes, OR, 1:20 in PBS) and mounted in ProLong Antifade Kit (Molecular Probes). All steps are performed at room temperature with three washes in PBS/2% BSA between incubations. Thrombin is added to the sample at selected times before the above fixing procedure is started in order to observe the effect on the organization of actin.

RESULTS

Evaluation of viscoelastic parameters of integrin receptor-actin linkages

Fibronectin-coated magnetic beads were attached to the surface of HUVEC. The beads can bind to fibronectin receptors such as integrins $\alpha_4\beta_1$, $\alpha_5\beta_1$, and/or $\alpha_V\beta_3$, and are thus, via the cytoplasmic domains of these integrins, indirectly connected to the actin cytoskeleton (Miyamoto et al., 1998). Fig. 1 shows a sequence of viscoelastic response curves induced by rectangular force pulses of 2 s duration with amplitudes of $f_0 = 600$ pN. The trajectories of the deflected beads were measured by a particle tracking tech-

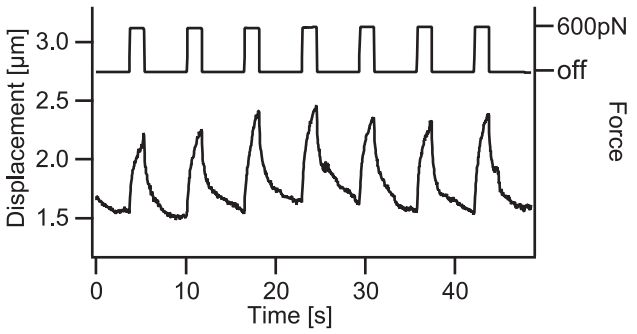

FIGURE 1 Sequence of force pulses (*top row*) of amplitude 600 pN and viscoelastic response curves (*bottom row*). The amplitudes of the bead deflection increase slightly during the first three pulses. Note that the beads return to the original position after the pulse, but that the decay curve exhibits a slowly decaying tail.

nique described previously (Ziemann et al., 1994) with an accuracy of ±10 nm. Nearly all of the response curves are reversible; this reversibility has been verified in numerous other experiments. By varying the force amplitude we have determined that for forces smaller that 2 nN we remain in the linear viscoelastic regime. However, closer inspection of Fig. 1 shows that, upon switching off the force, the relaxation of the bead toward the original position is considerably slower than the relaxation predicted by the response curve.

To provide further evidence for this finding, Fig. 2 *A* shows a single viscoelastic response curve at high resolution. The response curve exhibits three regimes: a fast elastic deflection (I), a curved region (II), where the elastic stress relaxes and the deflection appears to go over into a straight line regime, (III). The relaxation curve (IV) differs from the response curve. The corresponding decay time, τ_{decay}, is considerably larger than the relaxation time of the viscoelastic response. If regime III of the response curve is only due to viscous flow, then the bead should not relax to the original position, in contrast to the observed behavior. This discrepancy suggests that with the applied force pulses, the bead deflection is not associated with irreversible breakage or slippages of the actin network.

As described previously, the most straightforward (and simultaneously traditional) way to analyze the viscoelastic response curves in terms of viscoelastic parameters, such as the elastic storage modulus and the viscosity, is by adopting mechanical equivalent circuits that allow simulation of the observed curves. Following the principle of Occams Razor the simplest model enabling good fitting is considered as the best model for the quantitative interpretation of the data. In order to determine absolute values of the two-dimensional elastic moduli and the viscosities of the cell membrane, one has to measure the range of the deformation field in the membrane and apply the rigorous theory of elastic shells, as described previously (Bausch et al., 1998). In the present paper we restrict ourselves, however, to the evaluation of

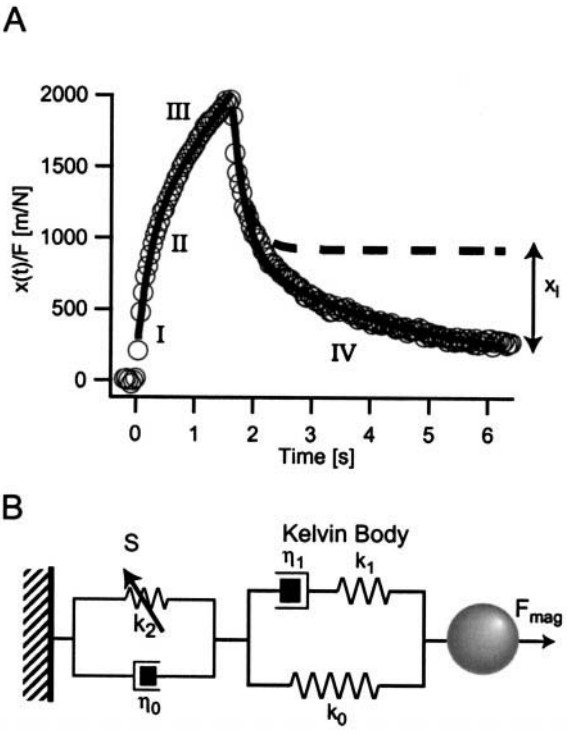

FIGURE 2 (*A*) Single viscoelastic response curve. The relaxation curve exhibits a slowly decaying regime and the corresponding decay time is considerably longer than the relaxation time of the response curve. The thick line corresponds to the viscoelastic response and relaxation function of the equivalent circuit composed of the Kelvin body in series with a dashpot. This circuit allows the fit of the response curve in an optimal way. However, to achieve optimal fit for the measured relaxation curve, the dashpot, η_0, must be replaced by a Voigt body (composed of the dashpot and an additional spring in series) with the additional relaxation time $\tau_{decay} = \eta_0/k_2$. (*B*) Equivalent circuit adopted for the formal analysis of the response and relaxation of the bead deflection, $x(t)$, in the direction of the magnetic field. The response is very well described by the equivalent circuit consisting of a Kelvin body (right side) and a dashpot in series, k_1 and k_0 are the spring constants, and η_0 and η_1 the viscosities. To account for the slow relaxation of the decay the dashpot on the left side is replaced by a parallel circuit of a dashpot (η_0) and a spring (k_2) in series, which yield a slow decay time $\tau_{decay} = \eta_0/k_2$. The transition between the response and the relaxation process is achieved by closing the switch S.

the experimental results in terms of the viscoelastic parameters of the simple equivalent models, which are relative measures of the membrane elasticity and viscosity.

We consider first the evaluation of the response curve. It is well-described in terms of the equivalent circuit shown in Fig. 2 *B* without the spring k_2. It consists of a so-called Kelvin (or Zener) body, which is composed of a parallel arrangement of a spring (spring constant k_0) and a series circuit of a spring (spring constant k_1) and a dashpot (viscosity η_1). To account for the straight line regime of the response curve, a dashpot (characterized by the viscosity η_0) is added to the Kelvin body in series.

As shown previously, the time-dependent deflection of the bead, $x(t)$, in the direction of the magnetic field is related to the external force according to

$$\frac{x(t)}{F(t)} = \frac{1}{k_0}\left(1 - \frac{k_1}{k_0 + k_1}\, e^{-(t/\tau)}\right) + \frac{t}{\eta_0} \qquad (1)$$

where τ is the relaxation time of the response curve and is given by

$$\tau = \frac{\eta_1(k_0 + k_1)}{k_0 k_1}$$

τ is called relaxation time because it corresponds to the average time required to relax the elastic stress in the viscoelastic body, which is mediated by the rearrangement of internal bonds. In reality, the relaxation process is determined by a distribution of relaxation times and τ is an average value. The elastic contribution to the deflection (regime I) is determined by the effective spring constant $k = (k_1 + k_0)$ according to $x(t) = F/k$. The last term on the right side of Eq. 1 describes the linear regime (III). By fitting Eq. 1 to the observed response function, the pertinent parameters k, τ, and η_0 are obtained.

Consider now the relaxation curve. It is reasonable to assume that the initial decay after disconnection of the magnetic force curve can be described by Eq. 1, neglecting the last term t/η_0. This would result in a transition to a constant value (denoted as x_1 in Fig. 2 *A*). The residual deflection, x_1, corresponds to the total displacement of the bead during the viscous flow (regime III). We can formally account for the observed slow decay of the bead to the original value by replacing the dashpot η_0 by a parallel arrangement of a dashpot, η_0, and a spring, with spring constant k_2. This can be achieved by closing of the switch S in Fig. 2 *B*, which corresponds to the introduction of a new, slow decay time: $\tau_{decay} \sim \eta_0/k_2$. The relaxation of the new equivalent circuit can be described as a superposition of the relaxations of the two systems in series

$$\frac{x(t)}{F(t)} = \frac{T}{\eta_0} + \frac{k_1}{k_0(k_0 + k_1)}\, e^{(t/\tau)} - \frac{1}{k_2}\,(1 - e^{(t/\tau_{decay})}) \qquad (2)$$

where T is the pulse duration and $\tau_{decay} = \eta_0/k_2$. (Note that the force is disconnected at $t = 0$.) Fitting the theoretical curve to the observed relaxation curve yields τ_{decay} and k_2. A perfect fit can be obtained as shown in Fig. 2 *A*.

Effect of thrombin on viscoelasticity of integrin-actin linkages

Fig. 3 shows an example of the effect of thrombin (0.1 units/ml) on the viscoelastic response of fibronectin-coated beads. A fast and dramatic decrease of the deformability of the bead-associated cell membrane was found within 5 s after thrombin stimulation, and this effect lasted for ~120 s. Even with the largest force possible (up to 5 pN) the bead could not be deflected. After this period, the membrane deformability recovered despite the continuous presence of thrombin.

Dose response experiments revealed that at a thrombin concentration of 0.05 units/ml 50% of the cells evaluated showed an effect. At higher concentrations all cells showed the same stiffening response, while below this threshold concentration no effect was observed. About 250 s after thrombin stimulation the amplitude and shape of the viscoelastic response curves were the same as before application of thrombin. Subsequent repeated application of thrombin had no further effect. However, the first visible response curve after recovery exhibits a different shape than the initial and fully recovered response curves, as shown in Fig. 4 *A*.

The application of cytochalasin D (10 μM), an agent that depolymerizes filamentous actin and prevents new actin polymerization, completely inhibited the effect of thrombin. Separate experiments (not shown) demonstrated that 4 min after cytochalasin D application, the actin network was completely disrupted. Even in the presence of thrombin the beads were deflected and membrane tethers were pulled.

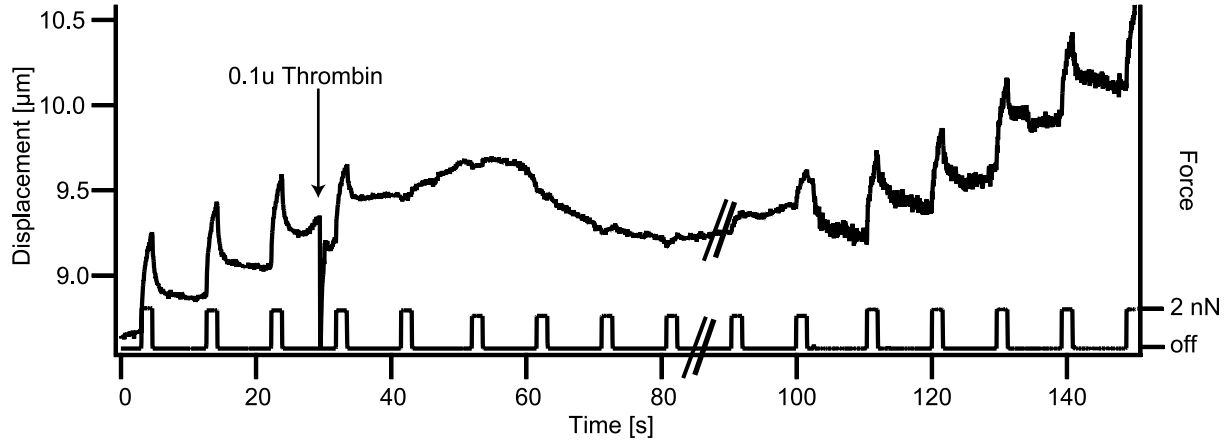

FIGURE 3 Effect of thrombin (0.1 units/ml) (time of injection marked by arrow) on viscoelastic response and relaxation curves of a magnetic bead coupled to integrin receptors through fibronectin coating. In order to illustrate the recovery of the deformability, the recording of the bead position is interrupted for 60 s, as indicated. Note that pulses were applied during the whole observation period. The sequence starts with pulse 1 and ends with 16.

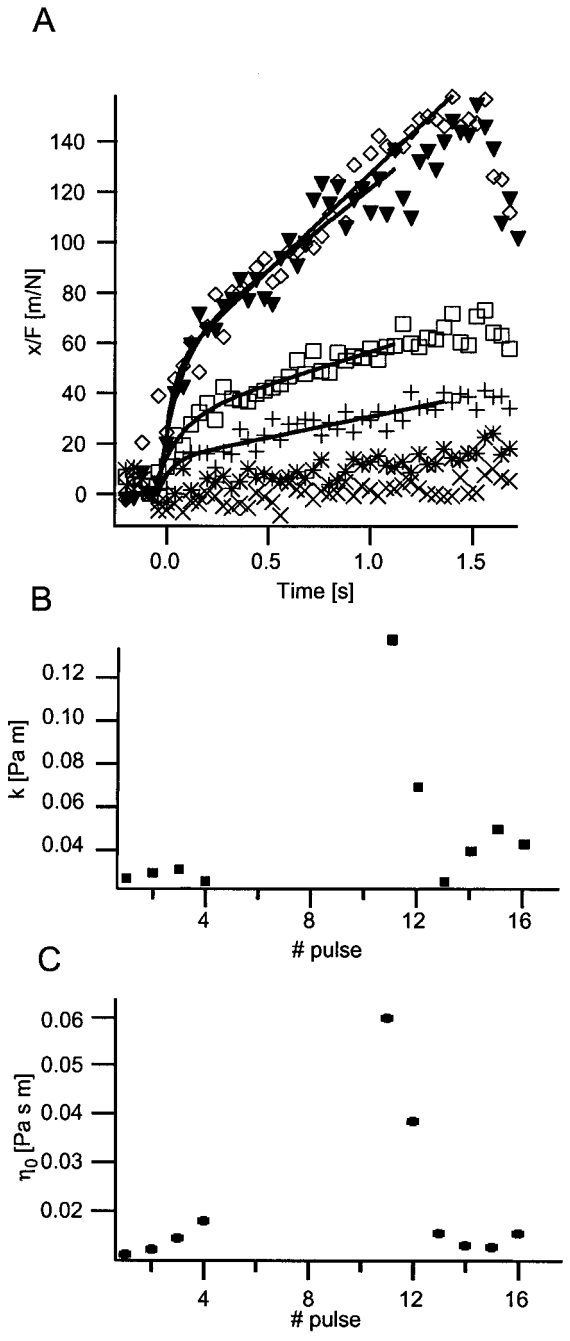

FIGURE 4 (*A*) Viscoelastic response curves at large resolution before (▼; ◇; pulses 2 and 3) and after (×; ∗; +; □; pulses 12–16) thrombin application. The respective fit functions are drawn with a thick line. (*B*) and (*C*) Viscoelastic parameters k and η_0 measured before (pulses 1–4) and after (pulses 12–16) addition of thrombin. The parameters were determined by fitting the equivalent circuit to the response function. As the pulses 5 to 10 did not deflect the attached bead, no parameters can be determined. The number on the abscissa corresponds to the number of the applied force pulse.

The effect of thrombin on the viscoelastic response may be evaluated more quantitatively by analyzing the response curves in terms of the equivalent circuit of Fig. 2 *B*. The values of the spring constants and viscosities are summarized in Fig. 4, *B* and *C*. The most remarkable findings of this data analysis are the drastically increased elastic moduli and viscosities immediately after thrombin application and the recovery to the original values in the presence of thrombin. Together, these data strongly suggest that above a threshold concentration thrombin induces a transient strong coupling of integrin receptors to the actin cortex, which relaxes completely within 250 s.

To relate the changes of the local viscoelastic behavior to changes of actin structure, the distribution of F-actin was observed at different times after addition of thrombin by staining with Alexa phalloidin. As shown in Fig. 5, stress fibers were formed within 2 s after stimulation. Although

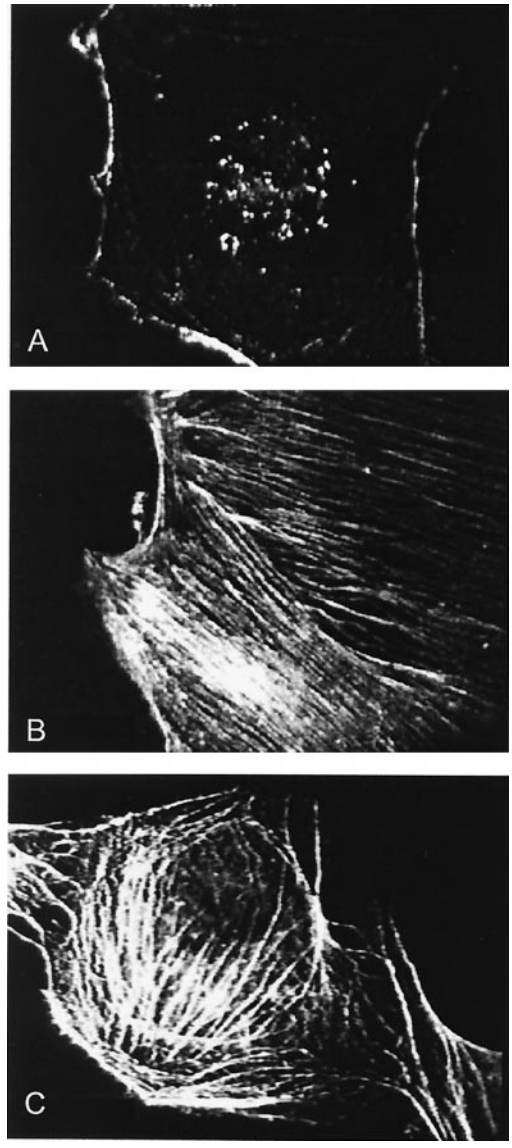

FIGURE 5 Fluorescence images of the actin network of the endothelial cells. In control experiments, only a few stress fibers were detectable (*A*) in a small fraction of cells. After the application of 0.1 units/ml thrombin for only 2 s the average density of stress fibers per cell drastically increased (*B*) and remained visible for >2 min (*C*).

stress fibers remained visible for up to 5 min, the stiffening response was reversible within 150 s. This observation shows that the applied thrombin induces a rapid reorganization of the actin cortex as reported also by previous workers (Garcia and Schaphorst, 1995). However, the rapid reversibility of the stiffening response is contrary to the longer lifetime of the stress fibers.

Stiffening response of collagen-coated beads

To investigate whether the thrombin-induced membrane stiffening depends on the type of integrin receptor to which the beads are coupled, experiments were performed with beads coated with collagen IV (not shown). Collagen binds to integrins such as $\alpha_1\beta_1$ or $\alpha_2\beta_1$. We found two major differences in the responses of collagen-coated beads as compared to the responses observed with fibronectin-coated beads. First, the average amplitudes of the viscoelastic response curves before application of thrombin were remarkably smaller. Second, thrombin exerted a much smaller stiffening effect. The deflection was not completely abolished, as in the case of beads coupled to fibronectin, while the recovery of the original membrane deformability was nearly the same.

Effect of lysophosphatidic acid on integrin-actin linkage: role of Ca^{2+} mobilization for the stiffening response

Lysophosphatidic acid (LPA) can simulate the effect of thrombin in HUVEC by inducing fast formation of stress fibers (Garcia and Schaphorst, 1995) that are dependent on Rho/Rho-kinase activation (Essler et al., 1999; Essler et al., unpublished results). In contrast to thrombin, LPA does not induce Ca^{2+} mobilization in HUVEC (Essler et al., unpublished results). We found that LPA elicited only a weak change of the viscoelastic response of the membrane: the spring constant decreased by ~10% and the viscosity η_0 increased by 10% (Fig. 6). This suggests that Ca^{2+} mobilization is not required, but may be cooperative for inducing the stiffening response.

To investigate the role of Ca^{2+} in the stiffening response induced by thrombin, we pretreated cells with both an intracellular calcium chelating reagent (BAPTA-AM) and an extracellular calcium chelating reagent (EGTA). The stiffening response of thrombin was still observed, even when both reagents were applied at the same time. This shows that neither intracellular nor extracellular calcium is necessary to evoke the observed stiffening response.

Effect of bacterial toxins that inactivate or activate the Rho/Rho-kinase pathway on the thrombin-stimulated stiffening response

Another major mechanism by which thrombin induces actin reorganization is through stimulation of the Rho/Rho-kinase pathway (Essler et al., 1998). In this pathway active Rho stimulates Rho-kinase, which phosphorylates and inactivates MLC-phosphatase. Reduced activity of MLC-phosphatase promotes enhanced MLC-phosphorylation, which in turn leads to actin-myosin interaction and bundling of filamentous actin into contractile fibers. To test the involvement of Rho in the stiffening response, we injected C3-transferase, a specific inhibitor of Rho, into the cells 1 h before addition of thrombin. In the C3-transferase-injected cells, thrombin exerted the same drastic reduction of the membrane deformability as in the absence of C3. Also, no detectable influence of C3 was observed if the toxin was added to the incubation medium for 24 h at a concentration of 10 μg/ml.

We next treated cells with the MLC-phosphatase inhibitor calyculin, which can induce stress fibers in HUVEC by causing MLC-dephosphorylation (Essler et al., 1998). Incubation of the cells with calyculin in concentrations up to 20 nM had no effect on the membrane elasticity. Moreover, calyculin did not influence the transient membrane stiffening effect of thrombin.

Finally, we treated cells with the cytotoxic necrotizing factor (CNF) of *Escherichia coli*, which in addition to Rho activates Rac and CDC42Hs and potentially other GTPases of the Rho family (Schmidt et al., 1997; Lerm et al., 1999). Treatment of cells with CNF (40 nM for 24 h) caused a maximal stiffening effect. We were not able to deflect the magnetic beads coupled to the membrane, as the membrane was already stiffer than we are able to measure. As expected, adding thrombin had no detectable effect. However, after applying cytochalasin D (10 μM) to the CNF-treated cells, deflections of the beads were observable and eventu-

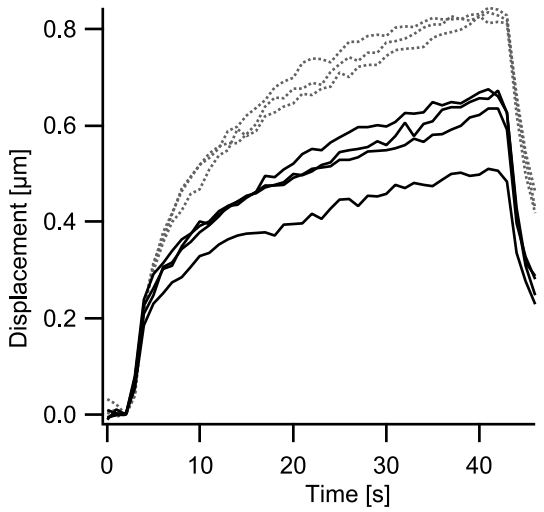

FIGURE 6 The effect of LPA on the viscoelastic response function. The response functions before the application of LPA are drawn with a dotted line; the response functions after the application are drawn with a solid line where the curve with the smallest amplitude corresponds to the first measurement after application of LPA. Note that the stiffening effect is much less pronounced than the effect observed with thrombin (cf. Fig. 4).

ally membrane tethers could be pulled. These data indicate that although intact actin polymerization is crucial, activation of Rho and induction of stress fibers alone are not responsible for the observed stiffening response induced by thrombin. However, the efficient induction of the stiffening response by CNF suggests involvement of another actin-regulating GTPase of the Rho family.

DISCUSSION

One major finding of the present work is that the application of magnetic bead microrheology technique enables real-time measurements of biochemically induced changes of the local deformability of cell membranes. By functionalizing the magnetic beads with macromolecules of the extracellular matrix, such as fibronectin or collagen, one can probe the association of distinct families of membrane receptors, such as the integrins, with the cytoskeleton and study the time evolution of changes caused by the stimulation of intracellular signaling pathways. The magnetic tweezers technique is non-invasive because the perturbation of the cells by the magnetic fields is small. This is an advantage compared to the complementary optical tweezers technique, where very high electrical fields in the optical wavelength regime are required, possibly causing local photodamage of cells (Ashkin, 1997). Further on, magnetic tweezers allow the application of much higher forces than would be possible using optical tweezers.

The analysis of the viscoelastic response curves in terms of mechanical equivalent circuits yields effective spring constants and viscosities. In order to relate these data to real shear elastic moduli μ and shear viscosities of the cell surface, one must solve the very complex problem of the elastic deformation of adherent cells under the action of a local shear force applied to the surface of the cell envelope. As has been shown previously for the case of fibroblasts, the solution can be approximated if the deformation field generated by a local force has a finite range (Bausch et al., 1998). It has been further shown that the range of the deformation field can be measured by observation of the local deflection of non-magnetic beads (1-μm diameter) coupled to the cell surface together with the magnetic tweezers. By application of the procedure, developed in the previous work, we found a value of $\mu^* = 10^{-4}$ Pa m for the surface shear elastic modulus of the HUVEC, which is a factor of 10 smaller than the value found for the 3T3 fibroblasts. Comparison of the values of μ^* and the corresponding spring constant $k = k_1 + k_0$ yields the relationship $\mu^* = 0.03k$. Thus, the spring constant is a reliable measure of the membrane elastic constant. Similarly, it has been shown that the effective viscosity, η, obtained from the data analysis in terms of the equivalent circuit can be related to the cytoplasmic viscosity of the cell. A similar analysis yields a cytoplasmic viscosity of 1×10^3 Pa s.

Comparative experiments performed with beads coupled to the membrane through fibronectin and collagen, respectively, show that in nearly all cases studied, the spring constant was systematically larger for collagen-coated beads. However, the thrombin-induced stiffening effect was much weaker. Fibronectin-coated beads have been shown to induce clustering of the fibronectin-specific integrin receptor $\alpha_5\beta_1$, which leads to the accumulation of seven actin binding proteins responsible for the formation of focal adhesion complexes (Miyamoto et al., 1995; Chicurel et al., 1998). Collagen does not exert such an effect and the microstructure of the cell envelope coupled to the force transducer is thus expected to be different.

A surprising result is that the recovery curves differ significantly from pulse to pulse, as a closer inspection of Figs. 1–3 shows. In particular, the shape of the response and the relaxation curve differ. Typically, the relaxation curves exhibit a more slowly decaying tail, corresponding to remarkably different response and relaxation time distributions. We formally account for this discrepancy by introducing an additional spring switched on during relaxation, which describes our results very well. We cannot relate this model to a detailed physical mechanism; however, such a behavior is expected if the local stress induces a transition of the linkage of the cytoplasmic domain of integrin to the actin network (e.g., through focal adhesion complexes) between two states, which are separated by an activation barrier. Such a transduction could be caused, for instance, by the breakage of weak reversible bonds within the linkage. Similar to the situation for chemical reactions, this would, in general, give rise to different transition times for the viscoelastic response and the relaxation processes.

The most intriguing result of the present study is the very strong local and fast stiffening of the membrane and the associated cytoskeleton near the cell surface receptors coupled to the magnetic bead. The analysis of the actin network by microfluorescence suggests that the thrombin effect is associated with the rapid formation of actin stress fibers. However, the presence of stress fibers lasted much longer than the stiffening effect, indicating that stress fiber formation alone does not provide the molecular basis for the observed effect. Moreover, the stiffening effect could not be prevented by inhibitors of Rho, which completely prevent formation of stress fibers. These two observations, together with the complete inhibition of the stiffening by cytochalasin D, suggest that the coupling of actin to the integrin receptors, and not the formation of stress fibers, is responsible for the stiffening.

In a recent study a complementary effect has been reported; by pulling membrane tethers it was demonstrated that PIP2 acts as a second messenger that regulates the adhesion energy between the cytoskeleton and the plasma membrane (Raucher et al., 2000). This new technique is also a very powerful tool to measure the coupling of the lipid membrane to the cytoskeleton; however, it does not allow

direct studies of the rearrangements within the cytoskeleton, which are possible by measuring the shear elastic moduli.

Consider now the biochemical implications of our findings. Numerous studies revealed that stimulation of actin reorganization by thrombin in endothelial cells is mediated by two signaling pathways exhibiting different response times (Garcia and Schaphorst, 1995; Essler et al., 1998). One pathway is initiated by the rapid increase of the intracellular Ca^{2+} concentration and the other by the somewhat slower stimulation of the Rho GTPase and its downstream effectors. The former response is mainly a consequence of opening of plasma membrane Ca^{2+} channels, but also of the rapid stimulation of phospholipase C (PLC), which triggers the cleavage of phosphatidyl-inositol-diphosphate (PIP2) into inositoltriphosphate (IP_3) and diacylglycerol (DAG). IP_3 induces the increase of the Ca^{2+} level by opening of intracellular Ca^{2+} storage vesicles. Together with calmodulin, Ca^{2+} stimulates the myosin light chain kinase (MLCK), which in turn causes the rapid phosphorylation of myosin light chains and thus activates this motor protein. The other pathway involves activation of the GTP-binding protein Rho followed by activation of Rho-kinase and deactivation of myosin light chain phosphatase (MLCP), which is responsible for the maintenance of a high level of activated myosin II through reduced dephosphorylation.

As shown by Garcia and Schaphorst (1995), the Ca^{2+} mobilization occurs within 60 s, while the response time of the MLC phosphorylation is ~100 s. The former time is comparable to the response time of the local membrane stiffening, whereas the time of the onset of the MLC phosphorylation corresponds well with the recovery time of the membrane stiffening (~100 s). However, our observations that extra and intracellular Ca^{2+} chelators do not prevent the stiffening effect, whereas lysophosphatidic acid, which does not stimulate a Ca^{2+} signal in HUVEC (Essler et al., unpublished), still induced a stiffening effect, are not compatible with the involvement of a Ca^{2+}-dependent pathway.

The Rho-based pathway can also be discarded as possible mechanism of the membrane stiffening for two reasons: first, because of the much longer response time, and second, because all effectors that inhibit the Rho-mediated pathway, such as the C3-toxin, do not affect the transient membrane stiffening.

Thus, the question of which signal pathway stimulated by thrombin is responsible for the transient stiffening of the integrin-actin linkages still remains. Our experiments with CNF might provide a clue, because CNF activates not only Rho, but other GTPases of the Rho family, such as Rac or CDC42Hs. Several important mechanisms have been described by which Rac and CDC42Hs can induce rapid actin polymerization. In thrombin-stimulated platelets Rac was shown to uncap actin filament barbed ends through phosphoinositide synthesis (Hartwig et al., 1995). Furthermore, Rac and CDC42Hs can activate proteins of the Wiskott Aldrich syndrome protein (WASP) family, which activate the Arp2/3 complex, a seven protein complex able to de novo nucleate actin filaments (Higgs and Pollard, 1999). Because actin seems to be required for the stiffening response, one of these pathways may be involved, a possibility that needs to be tested in future experiments.

In summary, we demonstrated that high-precision measurements of local viscoelastic moduli provide a new tool to study the effect of pathways on the membrane-associated cytoskeleton. We provided evidence that we gained valuable information that is complementary to that obtained by traditional techniques, such as microfluorescence of vital or fixed cells. The functionalization of the beads with different ligands allows the study of the coupling of distinct receptors to the cytoskeleton. Further studies will be necessary to understand the detailed mechanism and the role of the observed stiffening response of endothelial cells in response to thrombin.

This work was supported by the Deutsche Forschungsgemeinschaft (SFB 413). Financial support by the Fonds der Chemischen Industrie is also gratefully acknowledged. We thankfully acknowledge the excellent technical assistance of Gabriele Chmel.

REFERENCES

Aepfelbacher, M., M. Essler, E. Huber, A. Czech, and P. C. Weber. 1996. Rho is a negative regulator of human monocyte spreading. *J. Immunol.* 157:5070–5075.

Allen, W. E., G. E. Jones, J. W. Pollard, and A. J. Ridley. 1997. Rho, Rac and Cdc42 regulate actin organization and cell adhesion in macrophages. *J. Cell Sci.* 110:707–720.

Ashkin, A. 1997. Optical trapping and manipulation of neutral particles using lasers. *Proc. Natl. Acad. Sci. USA.* 94:4853–4860.

Bausch, A. R., W. Möller, and E. Sackmann. 1999. Measurement of local viscoelasticity and forces in living cells by magnetic tweezers. *Biophys. J.* 76:573–579.

Bausch, A. R., F. Ziemann, A. A. Boulbitch, K. Jacobson, and E. Sackmann. 1998. Local measurements of viscoelastic parameters of adherent cell surfaces by magnetic bead microrheometry. *Biophys. J.* 75: 2038–2049.

Bodmer, J. E., J. Van Engelenhoven, G. Reyes, K. Blackwell, A. Kamath, D. M. Shasby, and A. B. Moy. 1997. Isometric tension of cultured endothelial cells: new technical aspects. *Microvasc. Res.* 53:261–271.

Chicurel, M. E., R. H. Singer, C. J. Meyer, and D. E. Ingber. 1998. Integrin binding and mechanical tension induce movement of mRNA and ribosomes to focal adhesions. *Nature.* 392:730–733.

Essler, M., M. Amano, H. J. Kruse, K. Kaibuchi, P. C. Weber, and M. Aepfelbacher. 1998. Thrombin inactivates myosin light chain phosphatase via Rho and its target Rho kinase in human endothelial cells. *J. Biol. Chem.* 273:21867–21874.

Essler, M., M. Retzer, M. Bauer, J. W. Heemskerk, M. Aepfelbacher, and W. Siess. 1999. Mildly oxidized low density lipoprotein induces contraction of human endothelial cells through activation of Rho/Rho kinase and inhibition of myosin light chain phosphatase. *J. Biol. Chem.* 274: 30361–30364.

Garcia, J. G., and K. L. Schaphorst. 1995. Regulation of endothelial cell gap formation and paracellular permeability. *J. Invest. Med.* 43:117–126.

Hartwig, J. H., G. M. Bokoch, C. L. Carpenter, P. A. Janmey, L. A. Taylor, A. Toker, and T. P. Stossel. 1995. Thrombin receptor ligation and activated Rac uncap actin filament barbed ends through phosphoinositide synthesis in permeabilized human platelets. *Cell.* 82:643–653.

Higgs, H. N., and T. D. Pollard. 1999. Regulation of actin polymerization by Arp2/3 complex and WASP/Scar proteins. *J. Biol. Chem.* 274: 32531–32534.

Jalink, K., E. J. van Corven, T. Hengeveld, N. Morii, S. Narumiya, and W. H. Moolenaar. 1994. Inhibition of lysophosphatidate- and thrombin-induced neurite retraction and neuronal cell rounding by ADP ribosylation of the small GTP-binding protein Rho. *J. Cell Biol.* 126:801–810.

Kolodney, M. S., and R. B. Wysolmerski. 1992. Isometric contraction by fibroblasts and endothelial cells in tissue culture: a quantitative study. *J. Cell Biol.* 117:73–82.

Lampugnani, M. G., M. Corada, L. Caveda, F. Breviario, O. Ayalon, B. Geiger, and E. Dejana. 1995. The molecular organization of endothelial cell to cell junctions: differential association of plakoglobin, beta-catenin, and alpha-catenin with vascular endothelial cadherin (VE-cadherin). *J. Cell Biol.* 129:203–217.

Lerm, M., J. Selzer, A. Hoffmeyer, U. R. Rapp, K. Aktories, and G. Schmidt. 1999. Deamidation of Cdc42 and Rac by *Escherichia coli* cytotoxic necrotizing factor 1: activation of c-Jun N-terminal kinase in HeLa cells. *Infect. Immun.* 67:496–503.

Miyamoto, S., S. K. Akiyama, and K. M. Yamada. 1995. Synergistic roles for receptor occupancy and aggregation in integrin transmembrane function. *Science.* 267:883–885.

Miyamoto, S., B. Z. Katz, R. M. Lafrenie, and K. M. Yamada. 1998. Fibronectin and integrins in cell adhesion, signaling, and morphogenesis. *Ann. N.Y. Acad. Sci.* 857:119–129.

Raucher, D., T. Stauffer, W. Chen, K. Shen, S. L. Guo, J. D. York, M. P. Sheetz, and T. Meyer. 2000. Phosphatidylinositol 4,5-bisphosphate functions as a second messenger that regulates cytoskeleton-plasma membrane adhesion. *Cell.* 100:221–228.

Schmidt, G., P. Sehr, M. Wilm, J. Selzer, M. Mann, and K. Aktories. 1997. Gln 63 of Rho is deamidated by *Escherichia coli* cytotoxic necrotizing factor-1. *Nature.* 387:725–729.

Yamada, K. M., and B. Geiger. 1997. Molecular interactions in cell adhesion complexes. *Curr. Opin. Cell Biol.* 9:76–85.

Ziemann, F., J. Rädler, and E. Sackmann. 1994. Local measurements of viscoelastic moduli of entangled actin networks using an oscillating magnetic bead micro-rheometer. *Biophys. J.* 66:2210–2216.